3.96, 4.04, 4.14, 4.19, 4.24, 4.33, 4.41, 4.58 (m, 7 H), 4.48 (br m, 1 H), 5.23-5.33 (m, 1 H), 5.66 (br t, J = 12.6 Hz, 1 H), 6.49 (t, J = 12.6 Hz, 1 H), 6.66-7.73 (m, 30 H). **19** (minor isomer): ^{31}P NMR ($CDCl_3$ at -10 °C) δ 25.19 and 28.93 (AB q, J = 61.3 Hz). ^{1}H NMR ($CDCl_3$ at room temperature) δ 0.72 (br d, J = 5.8 Hz, 3 H), 1.47 (s, 3 H), 2.39-2.48 (br m, 1 H), 2.94-3.34 (m, 5 H), 3.96, 4.04, 4.14, 4.19, 4.24, 4.33, 4.41, 4.58 (m, 7 H), 4.89-4.98 (br m, 1 H), 5.23-5.33 (m, 1 H), 6.59 (t, J = 12.5 Hz, 1 H), 6.66-7.73 (m, 30 H).

The reaction of **19** with benzylamine at -10 °C was carried out in a similar manner to that of **17**. The enantiomeric purity of the product **4a** (72% yield) was determined to be 59.4%.

Acknowledgment. We thank the Yamada Science Foundation for partial financial support of this work.

Supplementary Material Available: Crystallographic data for palladium complex **15** and a table of anisotropic thermal parameters (2 pages); observed and calculated structure factors (24 pages). Ordering information is given on any current masthead page.

The Effect of Phenyl Ring Torsional Rigidity on the Photophysical Behavior of Tetraphenylethylenes

David A. Shultz and Marye Anne Fox*

Contribution from the Department of Chemistry, University of Texas at Austin, Austin, Texas 78712. *Received December 20, 1988*

Abstract: The synthesis and photochemical behavior of several members of the bis[n.1]metacyclophanylidene series are presented. The properties of these compounds are compared to a model compound, tetra-3-tolylethylene. The photophysical properties of the tethered tetraphenylethylenes change dramatically with the length of hydrocarbon tethers connecting the *gem*-phenyl rings. From these changes in photophysical properties and analysis of ground-state structures and properties, we propose that phenyl ring torsional motion plays a significant, if not primary, role in the photochemistry of tetraphenylethylenes.

Since photoexcitation involves the same orbitals as redox transformations, redox-induced geometric changes may be predicted by observing a molecule's photophysical properties. Electrochemical precedent[1] exists for geometrically linked multiple-electron transfers; therefore, one might expect that geometric changes induced by electronic excitation might control their redox properties as well. Tetraphenylethylenes are excellent models for testing this relationship because they are known to participate in multiple-electron redox reactions.[2,3]

To better understand the geometry changes that accompany deactivation of the singlet excited state of tetraphenylethylenes, we have synthesized and studied a class of torsionally restricted tetraphenylethylenes: the bis[n.1]metacyclophanylidenes ([n.1]MCs), Figure 1. Previously, we gave a brief account of the fluorescence properties of the [n.1]MCs (n = 4-6).[4] In this paper we describe in detail the synthesis, spectroscopic properties, and photophysical behavior of four torsionally restricted tetraphenylethylenes ([n.1]MCs: n = 4-7). The spectral properties are compared with those of tetraphenylethylene and/or tetra-*m*-tolylethylene (TTE).

Much of the discussion of the photophysical properties of the [n.1]MCs is related to the studies of the photochemical cis-trans isomerization of stilbenes,[5] a thoroughly investigated photochemical reaction. Indeed, details concering its mechanism continue to fascinate chemists.[6] Similarities between tetraphenylethylene and stilbene photochemistry exist primarily because of similarities in the nodal properties of their HOMOs and LUMOs. Both molecules are arylethylenes that exhibit olefinic bonding and essential single bond antibonding interactions in the HOMO, and olefinic antibonding and essential single bond bonding interactions in the LUMO. Therefore, changes in the geometry of these molecules, with respect to these bonds, will affect their energies in similar ways. Tetraphenylethylene is more akin to *cis*-stilbene than to the trans isomer, owing to phenyl ring torsion and steric repulsion of the *cis*-phenyl rings. This geometric likeness results in similar photophysics. Tetraphenylethylene, like *cis*-stilbene, has an exceedingly short singlet excited-state lifetime, a negligible fluorescence quantum yield (at room temperature in fluid solution), and a slow rate of intersystem crossing.

Our data indicate that the photophysical properties of tetraphenylethylenes change dramatically when hydrocarbon tethers connect *gem*-phenyl rings. In addition, the length of the chain determines the relative partitioning among deactivation pathways available to the singlet excited state. From these changes in photophysical properties and analysis of ground state structures and properties, we postulate that phenyl ring torsional motion plays a significant, if not primary, role in the photochemistry of tet-

(1) Britton, W. E. In *Topics in Organic Electrochemistry*; Fry, A. J., Britton, W. E., Eds.; Plenum Press: New York, 1986; p 227.
(2) Leigh, W. J.; Arnold, D. R. *Can. J. Chem.* **1981**, *59*, 3061.
(3) Fox, M. A.; Shultz, D. A., unpublished results.
(4) Shultz, D. A.; Fox, M. A. *Tetrahedron Lett.* **1988**, *29*, 4377.
(5) See the following reviews and references cited therein for discussions of the mechanism of photochemical cis-trans isomerization: (a) Salem, L.; Rowland, C. *Angew. Chem., Int. Ed. Engl.* **1972**, *11*, 92. (b) Saltiel, J.; D'Agostino, J.; Megarity, E. D.; Metts, L.; Neuberger, K. R.; Wrighton, M.; Zafiriou, O. C. *Org. Photochem.* **1973**, *3*, 1. (c) Salem, L. *Acc. Chem. Res.* **1979**, *12*, 87. (d) Saltiel, J.; Charlton, J. L. *Rearrangements in Ground and Excited States*; de Mayo, P., Ed.; Academic Press: New York, 1980; Vol. 3, p 25. (e) Hochstrasser, R. M. *Pure Appl. Chem.* **1980**, *52*, 2683. (f) Rettig, W. *Angew. Chem., Int. Ed. Engl.* **1986**, *25*, 971. (g) Bonacic-Koutecky, V.; Koutecky, J.; Michl, J. *Angew. Chem., Int. Ed. Engl.* **1987**, *26*, 170. (h) Malrieu, J. P.; Nebot-Gil, I.; Sánchez-Marín, J. *Pure Appl. Chem.* **1984**, *56*, 1241.
(6) For some recent studies of stilbene photophysics and photochemistry see the following and references cited therein: (a) Hamaguchi, H. *J. Phys. Chem.* **1989**, *93*, 7. (b) Ito, Y.; Kajita, T.; Kunimoto, K.; Matsuura, T. *J. Org. Chem.* **1989**, *54*, 587. (c) Petek, H.; Fujiwara, Y.; Kim, D.; Yoshihara, K. *J. Am. Chem. Soc.* **1988**, *110*, 6270. (d) Doany, F. E.; Hochstrasser, R. M.; Greene, B. I.; Millard, R. R. *Chem. Phys. Lett.* **1985**, *118*, 1. (e) Courtney, S. H.; Fleming, G. R. *J. Chem. Phys.* **1985**, *83*, 215. (f) Greene, B. I.; Scott, T. W. *Chem. Phys. Lett.* **1984**, *106*, 399. (g) Greene, B. I.; Scott, T. W. *Chem. Phys. Lett.* **1984**, *106*, 399. (h) Doany, F. E.; Heilweil, E. J.; Moore, R.; Hochstrasser, R. M. *J. Chem. Phys.* **1984**, *80*, 201. (i) Greene, B. I.; Farrow, R. C. *J. Chem. Phys.* **1983**, *78*, 3336. (j) Rothenberger, G.; Negus, D. K.; Hochstrasser, R. M. *J. Chem. Phys.* **1983**, *79*, 5360. (h) Hamaguchi, H.; Kato, T.; Tasumi, M. *Chem. Phys. Lett.* **1983**, *100*, 3. (i) Gustafson, T. L.; Roberts, D. M.; Chernoff, D. A. *J. Chem. Phys.* **1983**, *79*, 1559. (j) Amirav, A.; Jortner, J. *Chem. Phys. Lett.* **1983**, *95*, 295. (k) Knauss, D. C.; Evans, G. T. *J. Chem. Phys.* **1981**, *74*, 4627.

0002-7863/89/1511-6311$01.50/0

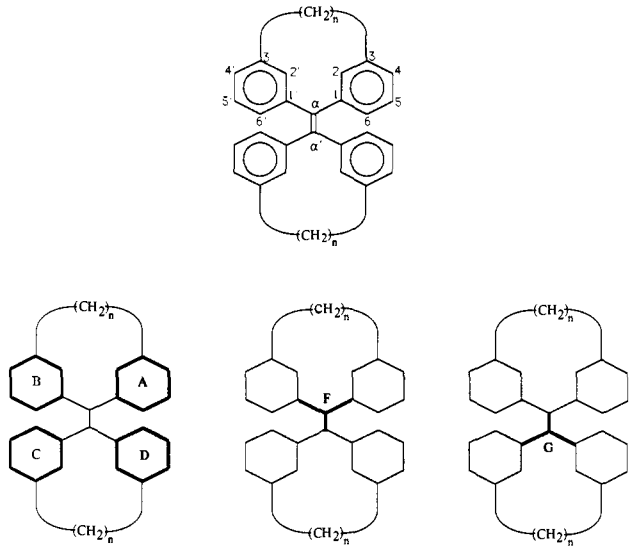

Figure 1. Numbering scheme of the [*n*.1]MCs (top). Atomic planes of the [*n*.1]MCs (bottom) are defined by the atoms whose bonds are outlined.

raphenylethylenes which is at least as important as torsion about the carbon–carbon double bond.

Experimental Section

Synthesis. The [*n*.1]MCs were obtained by the low-valent titanium coupling[7] of the corresponding [*n*.1]metacyclophanones **7a–d**, Scheme I and Figure 1. [4.1]Metacyclophan-11-one (**7a**) and [5.1]metacyclophane-12-one (**7b**) and their precursors have been synthesized previously,[8] while [6.1]metacyclophane-13-one (**7c**) and [7.1]metacyclophane-14-one (**7d**) are new compounds. These were prepared by pyrolysis of the corresponding bis-sulfones (**6a–d**) which were obtained by oxidation of the dithiacyclophanones using a procedure described by Atzmüller and Vögtle.[8] The dithiacyclophanones were obtained via a high-dilution reaction between α,ω-alkanedithiols and 3,3′-bis(bromomethyl)benzophenone (**4**). Compound **4** was obtained after deetherification of **3**. Intermediate **3** was produced by the Grignard reaction of **1** with nitrile **2** followed by acid hydrolysis. Yields for each step in the synthesis are shown in Scheme I. All preparations were carried out under an argon atmosphere.

(3-Bromophenyl)methyl Methyl Ether (1). 3-Bromobenzyl alcohol was methylated according to the procedure of Merz.[9] The crude product was distilled under reduced pressure to yield a colorless oil whose spectroscopic properties agreed with those reported in the literature,[10,11] bp 76–78 °C/0.5 Torr.

(3-Cyanophenyl)methyl Methyl Ether (2). Compound **2** was prepared by the reaction of **1** and CuCN according to the procedure of Friedman and Shechter.[12] The crude product was distilled under reduced pressure to yield a colorless oil whose spectroscopic properties agreed with those reported previously,[10,11] bp 80–83 °C/0.5 Torr.

3,3′-Bis(methoxymethyl)benzophenone (3). Compound **1** (71 g, 0.36 mol) in dry tetrahydrofuran (THF, 300 mL) was cannulated into a 4-L flask equipped with a mechanical stirrer and containing Mg turnings (8.8 g, 0.36 mol), two crushed-glass disposable pipets, and THF (350 mL) at a rate that maintained a vigorous reflux. The resulting Grignard reagent solution was heated under reflux for 1 h and was then stirred overnight at room temperature. (3-Cyanophenyl)methyl methyl ether (**2**, 52 g, 0.35 mol) in THF (250 mL) was added slowly via cannulation to the thick, green Grignard solution. The reaction mixture was heated at reflux for 4 h. Upon cooling to room temperature, a tan solid precipitated. THF (400 mL) was added, and the reaction mixture was refluxed for an additional 6 h. The reaction mixture was cooled to −15 °C with an ice/salt mixture and quenched with water (150 mL) followed by 40% HCl solution (250 mL). When all of the remaining metal appeared to have been consumed, the mixture was heated to 80 °C with stirring for

Scheme I

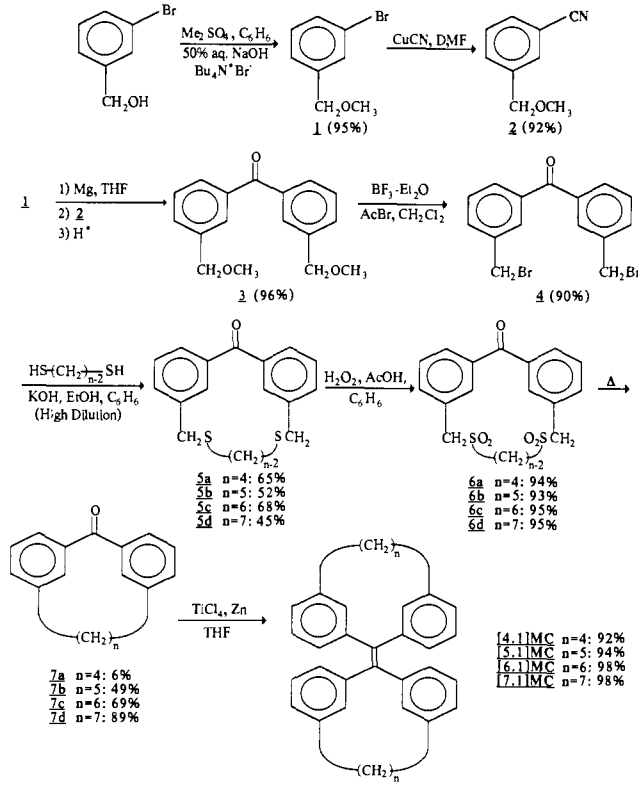

24 h. The reaction mixture was cooled and extracted with chloroform. The combined organic layers were washed sequentially with water, aqueous $NaHCO_3$, and saturated brine solutions, dried over Na_2SO_4, filtered, and then evaporated to dryness. The resulting light yellow oil was distilled under reduced pressure (bp 178–180 °C/0.05 Torr, lit.[8] 159–162 °C/0.01 Torr) to give 90.8 g 3,3′-bis(methoxymethyl)benzophenone **3**.

3,3′-Bis(bromomethyl)benzophenone (4). To a stirred solution of **3** (91 g, 0.34 mol) in methylene chloride (500 mL) at 0 °C was added sequentially BF_3–etherate (250 mL, 2.0 mol) and acetyl bromide (140 mL, 2.0 mol). Upon warming to room temperature, a cream-colored solid precipitated. An additional 150 mL of methylene chloride was added and the mixture was refluxed for 4 h, cooled to −5 °C, and quenched by the cautious addition of 10% aqueous $NaHCO_3$ solution. The reaction mixture was transferred to a separatory funnel and diluted with methylene chloride. The layers were separated, and the organic layer was washed with water and saturated brine, dried over Na_2SO_4 and concentrated to dryness. The resulting light tan solid was recrystallized from benzene to give 111 g of a white, crystalline solid, mp 149–150 °C (lit.[8] 149–151 °C).

General Procedure for the Preparation of the Dithia[*n*.1]metacyclophanones (5a–d). Solutions of 3,3′-bis(bromomethyl)benzophenone (**4**, 30 mmol) in THF (to give 280 mL) and the corresponding α,ω-alkanedithiol (30 mmol) plus KOH (35 mmol) in 90% ethanol (to give 280 mL) were added simultaneously, via motor-driven syringe pump, to vigorously stirred, refluxing benzene (1200 mL) and 95% ethanol (1200 mL) over a period of 10 h. Following the addition, the yellow reaction mixture was heated for an additional 4 h and was then concentrated by simple distillation. The residue was taken up in methylene chloride and washed with water, dried over Na_2SO_4, and evaporated to yield a yellow semisolid which was recrystallized from chloroform or ethyl acetate.

2,7-Dithia[8.1]metacyclophan-15-one (5c). The product was recrystallized from chloroform, mp 157–158 °C; ^{1}H NMR (300 MHz, $CDCl_3$) δ 1.71 (m, 4 H), 2.42 (m, 4 H), 3.69 (s, 4 H), 7.41 (s, 2 H), 7.53 (t, J = 7.6 Hz, 2 H), 7.60 (d, J = 7.8 Hz, 2 H), 7.86 (d, J = 7.5 Hz, 2 H); ^{13}C NMR (300 MHz, $CDCl_3$) δ 28.04, 29.94, 34.75, 128.00, 129.62, 130.66, 133.05, 137.94, 138.38, 196.85; MS (EI) 328 (M^+), 242, 207, 180, 165, 119, 90; HRMS (EI) m/z calc = 328.095 56, m/z meas = 328.096 00.

2,8-Dithia[9.1]metacyclophan-16-one (5d). The product was recrystallized from ethyl acetate, mp 150–152 °C; ^{1}H NMR (300 MHz, $CDCl_3$) δ 1.37 (m, 2 H), 1.47 (p, J = 7.1 Hz, 4 H), 2.37 (t, J = 7.2 Hz, 4 H), 3.71 (s, 4 H), 7.50 (m, 4 H), 7.58 (d, J = 7.7 Hz, 2 H), 7.82 (d, J = 7.5 Hz, 2 H); ^{13}C NMR (300 MHz, $CDCl_3$) δ 27.60, 28.89, 30.79, 35.82, 127.55, 129.16, 130.43, 132.68, 138.21, 139.04, 196.78; MS (EI)

(7) Mukiyama, T.; Sato, T.; Hanna, J. *Chem. Lett.* **1973**, 1041.
(8) Atzmüller, M.; Vögtle, F. *Chem. Ber.* **1978**, *111*, 2547.
(9) Merz, A. *Angew. Chem., Int. Ed. Engl.* **1973**, *12*, 846.
(10) Tomioka, H.; Tabayashi, K.; Ozaki, Y.; Izawa, Y. *Tetrahedron* **1985**, *41*, 1435.
(11) Montheard, J. P.; Camps, M.; Chatzopoulos, M.; Pham, Q. T. *Makromol. Chem.* **1985**, *186*, 2513.
(12) Friedman, L.; Shechter, H. *J. Org. Chem.* **1961**, *26*, 2522.

342 (M^+), 241, 207, 179, 165, 101, 90.

2,7-Dithia[8.1]metacyclophan-15-one 2,2,7,7-Tetraoxide (6c). Compound **6c** was prepared by the oxidation of dithiacyclophanone **5c** with H_2O_2/AcOH according to the published procedure;[8] ^{1}H NMR (90 MHz, d_6-DMSO, TMS) δ 1.99 (p, J = 7.3 Hz, 2 H), 3.30 (m, 4 H), 4.63 (s, 4 H), 8.03–7.56 (m, 8 H).

2,8-Dithia[9.1]metacyclophan-16-one 2,2,8,8-Tetraoxide (6d). Bis-sulfone **6d** was prepared by the oxidation of dithiacyclophanone **5d** by the published procedure;[8] ^{1}H NMR (90 MHz, d_6-DMSO, TMS) δ 1.50 (m, 6 H), 2.93 (m, 4 H), 4.52 (s, 4 H), 8.10–7.60 (m, 8 H).

General Procedure for the Pyrolysis of the Dithia[*n*.1]metacyclophanone Tetraoxides (6a–d). Portions of the bis-sulfones (**6a–d**, ca. 200 mg) were pyrolyzed by passage through a heated (ca. 600 °C) quartz tube (60 cm × 1 cm i.d.) that was loosely packed (one-third of the length) with quartz chips. Pyrolysis without the quartz chips resulted in the formation of large amounts of the mono-SO_2 extrusion product for compounds **6b–d**. The exit end of the quartz tube was attached to two liquid N_2 cooled traps and a high-vacuum line (ca. 10^{-5} Torr). Typically, the pyrolysate condensed on the quartz tube just outside the oven within 5 min of moving the oven over the section of the pyrolysis tube containing the bis-sulfone. After the pyrolysis tube cooled to room temperature, the crude product was washed from the surface with chloroform. The washings were combined and evaporated to dryness. The resulting residue was then recrystallized from 95% ethanol or methanol.

[6.1]Metacyclophan-13-one (7c). The light yellow crystalline pyrolysate was purified by recrystallization from methanol, mp 75–77 °C; ^{1}H NMR (300 MHz, $CDCl_3$) δ 1.30 (m, 4 H), 1.73 (m, 4 H), 2.67 (dd, J = 6.4, 6.1 Hz, 4 H), 7.24 (s, 2 H), 7.36 (d, J = 7.5 Hz, 2 H), 7.46 (dd, J = 7.5, 7.6 Hz, 2 H), 7.79 (d, J = 7.6 Hz, 2 H); ^{13}C NMR (300 MHz, $CDCl_3$) δ 24.47, 29.76, 32.12, 125.77, 128.93, 132.26, 134.65, 137.83, 139.67, 197.47; MS (EI) 264 (M^+), 207, 179, 165, 118, 90, 77.

[7.1]Metacyclophan-14-one (7d). A light yellow partially crystalline pyrolysate was obtained which was purified by recrystallization from ethanol, mp 117–118 °C; ^{1}H NMR (300 MHz, $CDCl_3$) δ 1.32 (m, 6 H), 1.70 (br m, 4 H; 2.74 (dd, J = 5.9, 5.8 Hz, 4 H), 7.35 (d, J = 7.4 Hz, 2 H), 7.40 (s, 2 H), 7.44 (t, J = 7.5 Hz, 2 H), 7.81, d, J = 7.6 Hz (2 H); ^{13}C NMR (300 MHz, $CDCl_3$) δ 25.36, 26.14, 27.73, 33.61, 126.25, 128.69, 129.13, 133.47, 138.23, 140.33, 197.53; MS (EI) 278 (M^+), 209, 179, 165, 118, 90, 41.

General Procedure for the Preparation of the [*n*.1]MCs. Typically, Zn dust (200 mg, 3.0 mmol) was added in one portion to a stirred solution of $TiCl_4$ (0.16 mL, 1.5 mmol) in tetrahydrofuran (THF, 20 mL) at −78 °C. Upon warming to room temperature, the reaction mixture turned dark brown–purple and then black. This mixture was heated under reflux for 1 h and was then cooled to room temperature. The [*n*.1]metacyclophanone **6** (0.9 mmol) in dry THF (20 mL) was added, and the reaction mixture was gently heated under reflux for 4 h, cooled to 0 °C, and then quenched by the careful addition of 10% aqueous Na_2CO_3 (50 mL). The resultant black emulsion was filtered through glass wool into a separatory funnel, and the filter cake was washed copiously with $CHCl_3$. This solution was washed sequentially with water (100 mL), 50% HCl (100 mL), and saturated brine (100 mL). The organic layer was dried over Na_2SO_4, filtered, and evaporated to dryness. The solid residue contained only one mobile product on thin-layer chromatography (silica gel/benzene). The [*n*.1]mCs were purified by recrystallization from chloroform/ethanol, followed by fractional thermal gradient sublimation. Crystals of [5.1]MC and [6.1]MC suitable for X-ray analysis were obtained from slow evaporation of a benzene solution. Fractional thermal gradient sublimation yielded X-ray quality crystals of [4.1]MC and [7.1]MC.

Bis[4.1]metacyclophanylidene ([4.1]MC). The crude product was recrystallized from chloroform/ethanol, mp 319.4 °C; ^{1}H NMR (300 MHz, $CDCl_3$) δ 1.04 (m, 4 H), 1.65 (m, 4 H), 2.21 (m, 4 H), 2.82 (m, 4 H), 6.39 (s, 4 H), 6.87 (d, J = 7.5 Hz, 4 H), 6.99 (t, J = 7.5 Hz, 4 H), 7.39 (d, J = 7.5 Hz, 4 H); ^{13}C NMR (300 MHz, $CDCl_3$) δ 24.75 (C–HB), 33.33 (C–B), 126.40 (C-5), 128.56 (C-4), 128.56 (C-6), 136.33 (C-2), 136.65 (C-α), 139.69 (C-1), 148.59 (C-3); UV (THF) λ_{max} (ϵ, L/mol cm) 230 (22 000), 250 (16 300), 344 nm (15 600); IR (KBr wafer) 3015 (m), 2900 (s), 2860 (s), 1595 (s), 1570 (mw), 1560 (mw), 1540 (w), 1440 (m), 1415 (m), 1370 (m), 1360 (mw), 1345 (w), 1310 (w), 1260 (m), 1225 (w), 1160 (m), 1090 (s), 1045 (ms), 1020 (ms), 935 (ms) cm^{-1}; Raman 1586, 1564, 1306 cm^{-1}; MS (EI) 440 (M^+). Anal. Calcd for $C_{34}H_{32}$: C, 92.68; H, 7.32. Found: C, 92.82; H, 7.56.

Bis[5.1]metacyclophanylidene ([5.1]MC). The crude product was recrystallized from chloroform/ethanol, mp 348.3 °C, ^{1}H NMR (300 MHz, $CDCl_3$) δ 0.97 (pent, J = 7.2 Hz, 4 H), 1.31 (m, 8 H), 2.37 (dd, J = 5.8, 6.0 Hz, 8 H), 6.58 (s, 4 H), 6.79 (d, J = 7.7 Hz, 4 H, 6.91 (t, J = 7.6 Hz, 4 H), 7.16 (d, J = 7.7 Hz, 4 H); ^{13}C NMR (300 MHz, $CDCl_3$) δ 23.75 (C–BHB), 30.36 (C–HB), 34.79 (C–B), 127.17 (C-6), 127.27 (C-5), 129.26 (C-4), 134.68 (C-2), 137.81 (C-α), 141.11 (C-1), 146.45 (C-3); UV (THF) λ_{max} (ϵ, L/mol cm) 252 (15 734), 340 nm (12 987); IR (KBr wafer) 3010 (m), 2920 (s), 2850 (s), 1595 (s), 1575 (mw), 1558 (w), 1480 (m), 1460 (m), 1440 (m), 1420 (m), 1340 (mw), 1320 (mw), 1295 (w), 1260 (w), 1240 (w), 1150 (mw), 1120 (mw), 1090 (mw), 1070 (mw), 1050 (mw), 1018 (mw), 920 (m), 820 (mw), 800 (ms), 780 (ms), 710 (s), 725 (s), 640 (w), 690 (w) cm^{-1}. Raman 1596, 1574, 1306 cm^{-1}; MS (EI) 468 (M^+). Anal. Calcd for $C_{36}H_{36}$: C, 92.26; H, 7.68. Found: C, 89.44; H, 7.68. HRMS (EI) m/z calcd = 468.281 88; m/z measd = 468.282 00.

Bis[6.1]metacyclophanylidene ([6.1]MC). The crude product was recrystallized from chlofoform/ethanol, mp 337.4 °C; ^{1}H NMR (300 MHz, $CDCl_3$) δ 0.89 (br s, 8 H), 1.52 (br s, 8 H), 2.40 (two br s, 8 H), 6.60 (s, 4 H), 6.82 (d, J = 7.6 Hz, 4 H), 6.91 (t, J = 7.6 Hz, 4 H), 7.06 (d, J = 7.5 Hz, 4 H); ^{13}C NMR (300 MHz, $CDCl_3$) δ 24.47 (C–BHB), 31.14 (C–HB), 33.00 C–B), 126.26 (C–6), 127.49 (C–5), 129.99 (C–4), 134.75 (C–2), 138.89 (C–α), 140.86 (C–1), 145.03 (C–3); UV (THF) λ_{max} (ϵ, L/mol cm) 252 (20 580), 340 nm (13 943); IR (KBr wafer) 3000 (m), 2890 (s), 2830 (s), 1600 (s), 1578 (m), 1483 (ms), 1440 (ms), 1420 (m), 1350 (m), 1340 (mw), 1310 (w), 1280 (mw), 1238 (w), 1180 (mw), 1160 (mw), 1140 (w), 1090 (m), 1060 (mw), 1010 (mw) 974 (w), 912 (m), 820 (m), 800 (s), 710 (s), 765 (m), 740 (m), 730 (ms), 710 (s), 700 (ms), 650 (w) cm^{-1}; Raman 1593, 1568, 1304 cm^{-1}; MS (EI) 496 (M^+). Anal. Calcd for $C_{38}H_{40}$: C, 91.88; H, 8.12. Found: C, 91.51; H, 8.18.

Bis[7.1]metacyclophanylidene ([7.1]MC). The crude product was recrystallized from chloroform/ethanol, mp 320.6 °C; ^{1}H NMR (300 MHz, $CDCl_3$) δ 0.94 (m, 8 H), 1.12 (pent, J = 6.0 Hz, 4 H), 1.36 (m, 8 H), 2.52 (br s, 8 H), 6.77 (s, 4 H), 6.83 (d, J = 6.9 Hz, 4 H), 6.91 (dd, J = 7.3, 7.6 Hz, 4 H), 6.97 (d, J = 7.3 Hz, 4 H); ^{13}C NMR (300 MHz, $CDCl_3$) δ 25.17 (C–THB), 27.83 (C–BHB), 28.47 (C–HB), 35.11 (C–B), 126.91 (C–6), 127.75 (C–5), 129.54 (C–4), 131.40 (C–2), 140.11 (C–α), 141.53 (C–1), 145.07 (C–3); UV (tHF) λ_{max} (ϵ, L/mol cm) 252 (17 200), 326 nm (11 920); IR (KBr wafer) 3025 (m), 2920 (s), 2850 (s), 1605 (ms), 1585 (m), 1490 (ms), 1465 (m), 1450 (ms), 1430 (m), 1370 (w), 1310 (w), 1290 (w), 1270 (w), 1175 (m), 1100 (m), 1080 (m), 1010 (mw) 990 (w), 915 (s), 805 (s), 740 (s), 730 (s), 712 (s) cm^{-1}; Raman: 1593, 1568, 1304 cm^{-1}; MS (EI) 524 (M^+). Anal. Calcd for $C_{40}H_{44}$: C, 91.55; H, 8.45. Found: C, 88.81; H, 8.15. HRMS (EI) m/z calcd = 524.344 52; m/z measd = 524.345 00.

Methods. Fluorescence spectra were recorded on a SLM-Aminco SPF-500C spectrofluorometer. The emission spectra were corrected for photomultiplier tube response, and the excitation spectra were corrected for the excitation source profile. The sample cell was a 1-cm square cuvette attached to a stopcock which allowed for freeze–pump–thaw degassing of the contents. The low temperatures required for variable-temperature measurements were obtained by controlling the flow of liquid N_2 into a quartz Dewar in which the sample cell was clamped. Temperatures were determined with a calibrated thermocouple. At each measured temperature, the degassed sample was allowed to equilibrate until the measurements became reproducible (ca. 10 min). The solvent, 2-methyltetrahydrofuran, was distilled from lithium aluminum hydride prior to use. THF was distilled from sodium metal prior to use. Fluorescence quantum yields (Φ_f) were calculated by using 9,10-diphenylanthracene (Φ_f = 0.95)[13] as reference. All solutions had matched optical densities (0.10 ± 0.01) at the excitation wavelength (350 nm). UV–vis absorption spectra (THF solvent) were recorded on a Hewlett Packard HP 8450A diode array spectrometer.

Time-resolved emission and absorption spectroscopies were performed at the Center for Fast Kinetics Research (CFKR) at the University of Texas at Austin. The time-resolved data are the results of at least three experiments consisting of approximately 35 laser shots each. Time-resolved emission data (λ_{obs} = 450 nm) were collected by using a streak camera after excitation of the samples with the third harmonic (355 nm) of a mode-locked Nd:YAG laser (Quantel YG402, 30-ps pulse). All solutions had optical densities of 0.2 ± 0.06 (<10^{-5} M in THF) at the excitation wavelength. The experimental arrangement has been described previously.[14] In addition, the fluorescence lifetime of [4.1]MC was measured by single-photon counting (350-nm excitation, instrument response function = 300 ps). This experimental arrangement has been described elsewhere.[15] Picosecond absorption spectra[16] were collected at several different delay times (prepulse to 1.2 ns) between exciting (355 nm) and analyzing pulses. All solutions had optical densities of 1.5 ± 0.2 (<10^{-4} M in THF or aqueous THF) at the excitation wavelength and were cycled through a 1 × 0.2 cm flow cell by a peristaltic pump. The same laser was used as that for the streak camera experiments. Data

(13) Maciejewski, A.; Steer, R. P. *J. Photochem.* **1986**, *35*, 59.
(14) Rodgers, M. A. J. *Chem. Phys. Lett.* **1981**, *78*, 509.
(15) Atherton, S. J.; Beaumont, P. C. *J. Phys. Chem.* **1986**, *90*, 2252.
(16) Atherton, S. J.; Hubig, S. M.; Callan, T. J.; Duncanson, J. A.; Snowden, P. T.; Rodgers, M. A. J. *J. Phys. Chem.* **1987**, *91*, 3137.

Table I. Aromatic Proton NMR Chemical Shifts for the [n.1]MCs[a]

	δ			
cmpd	H-2	H-4	H-5	H-6
[4.1]MC	6.39	6.87	6.99	7.39
[5.1]MC	6.58	6.79	6.91	7.16
[6.1]MC	6.60	6.82	6.91	7.06
[7.1]MC	6.77	6.83	6.91	6.97
TTE	6.83	6.82	6.97	6.89

[a] Spectra were recorded at 300 MHz in deuteriochloroform.

from all experiments were manipulated on a PDP 11/70 minicomputer and analyzed by previously described methods.[17] The laser intensity was constant throughout the measurements, and all rate constants were independent of the laser intensity, which was typically <2 mJ/cm^2.

Single-crystal Raman spectra were recorded on a Nicolet 60-SZR FT-Raman spectrometer using 1060-nm excitation. Infrared spectra (KBr wafers) were recorded on a Beckman AccuLab 8 infrared spectrometer.

^{1}H and ^{13}C NMR spectra were recorded on General Electric GN 500 and QE 300 spectrometers or on a Varian EM 390 instrument. Variable-temperature spectra were recorded on a General Electric GM 500 spectrometer. ^{1}H and ^{13}C NMR chemical shifts of the [n.1]MCs were assigned with the aid of ^{1}H COSY,[18] ^{1}H NOE difference, and CH COSY[19] experiments. Chemical shifts are reported in ppm, downfield from the internal standard tetramethylsilane.

Elemental analyses were performed by Galbraith Laboratories, Knoxville, TN. High-resolution mass spectra (EI) were recorded on a CEC 21-110 high-resolution mass spectrometer. The melting points of the [n.1]MCs were determined via differential scanning calorimetry using a Perkin-Elmer 7 Series thermal analysis system. All of the [n.1]MCs showed only one sharp, endothermic phase transition (the melting point) between room temperature and ca. 450 °C, the temperature at which the onset of decomposition occurred.

Force field calculations were carried out by using MM2.[20] Relative strain energies were obtained by subtracting the strain energy of an alkylated tetraphenylethylene from the corresponding [n.1]MC. Specifically, the strain energies of tetrakis(3-ethylphenyl)ethylene, *trans*-[bis(3-ethylphenyl)bis(3-*n*-propylphenyl)]ethylene, tetrakis(3-*n*-propylphenyl)ethylene, and *trans*-[bis(3-*n*-propylphenyl)bis(3-*n*-butylphenyl)]ethylene were calculated and subtracted from those calculated for [4.1]MC, [5.1]MC, [6.1]MC, and [7.1]MC, respectively. The aromatic contribution to the strain energy was estimated by removing the hydrocarbon tethers, adding hydrogens, and recalculating the strain energy using only one iteration. The resulting value was then divided by the total strain energy.

Results

Ground-State Effects. A. NMR Spectra. Table I lists the chemical shifts of the aromatic protons of the [n.1]MCs and TTE. The chemical shift of the "inner" aromatic protons (H-2, Figure 1) moves to higher field as the hydrocarbon tethers are shortened. All four tether proton signals of [4.1]MC are fully resolved at room temperature. The chemical shifts of the aromatic protons for all of the [n.1]MCs as well as those of the hydrocarbon tethers of [4.1]MC are temperature independent between 26 and −80 °C.[21] However, the chemical shifts of the tether protons of [5.1]MC, [6.1]MC, and [7.1]MC do show temperature dependence over this range. Table II lists these changes. Since neither the chemical shifts nor the coupling constants of the tether protons of [4.1]MC are temperature dependent, they are not included in Table II. The benzylic (B) proton signals of [5.1]MC appear as a triplet over the entire temperature range. However, the B proton signals of [6.1]MC and [7.1]MC coalesce slightly below room temperature and appear as separate resonances at lower temperatures. In addition, the homobenzylic (HB) proton signals of [5.1]MC and the bishomobenzylic (BHB) proton signals of [7.1]MC coalesce at low temperatures and appear as separate resonances at ca. −15 and −40 °C, respectively (Table II).

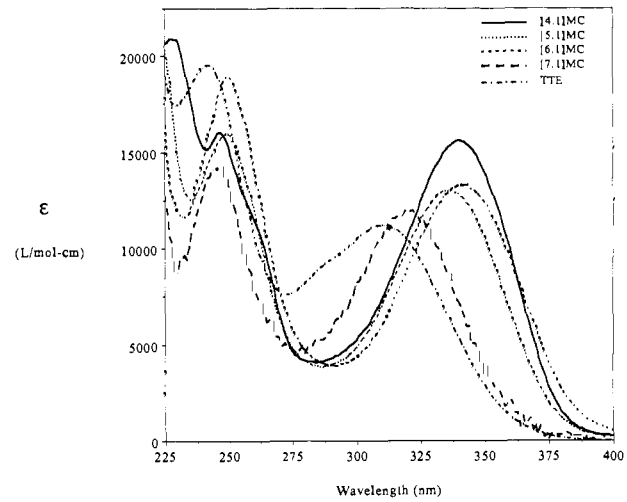

Figure 2. Ground-state absorption spectra of the [n.1]MCs and TTE.

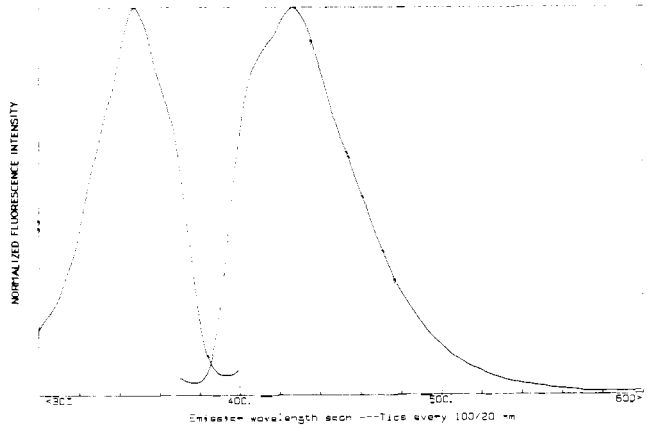

Figure 3. Fluorescence excitation and emission spectra of [4.1]MC recorded at 77 K.

B. X-ray Crystal Structures. The crystal structures of the [n.1]MCs were determined by X-ray diffraction techniques. Values of several torsional angles, ϕ, bond lengths, r, and angles, ϑ, are shown in Tables III and IV. Values of these parameters for tetraphenylethylene are included for comparison.[22] Figure 1 shows the numbering scheme that defines these values.

These data show that the phenyl ring torsional angles and the *gem*-phenyl ring bond angles $\vartheta(1\text{-}\alpha\text{-}1')$ decrease with decreasing tether size. [4.1]MC, [5.1]MC, and [6.1]MC exhibit ethylenic torsional angles (ϕ_{FG}) approximately twice that of tetraphenylethylene.[22] The olefinic torsional angle of [7.1]MC is closer to that of tetraphenylethylene than to the other cyclophanes.[23]

C. Vibrational Spectra. Both the Raman and IR spectra of the cyclophanes were measured and compared to that of tetraphenylethylene. The Raman spectrum of $^{13}C_{\alpha},C_{\alpha'}$-tetraphenylethylene[24] was also recorded to assign vibrational frequencies to specific vibrational modes. Specifically, we assign the signals at 1564 and ca. 1305 cm^{-1} [25] in the spectrum of tetraphenylethylene to the symmetric ethylenic stretch ($\nu_{\alpha-\alpha'}$) and the $1\text{-}\alpha$ stretches ($\nu_{1-\alpha}$), respectively. Assignments are based on the low-frequency shift of these stretching modes upon ^{13}C isotopic substitution.[26]

The $\nu_{\alpha-\alpha'}$ stretching frequencies for the cyclophanes (ca. 1570 cm^{-1}) are slightly higher than that of tetraphenylethylene, while the $\nu_{1-\alpha}$ stretching frequencies (ca. 1300 cm^{-1}) are slightly lower.

(17) Foyt, D. C. *Comput. Chem.* **1981**, *5*, 49.
(18) Bax, A.; Freeman, R.; Morris, G. *J. Magn. Reson.* **1981**, *42*, 164.
(19) Bax, A.; Morris, G. *J. Magn. Reson.* **1981**, *42*, 501.
(20) (a) Allinger, N. L. *J. Am. Chem. Soc.* **1977**, *99*, 8127. (b) QCPE Program No. 395.
(21) All proton chemical shifts of [4.1]MC are unaffected by temperatures up to 90 °C (spectra recorded in d_8-toluene at 500 MHz).
(22) Hoekstra, A.; Vos, A. *Acta Crystallogr., Sect. B* **1975**, *31*, 1722.
(23) X-ray studies show no pyramidalization of the olefinic carbons of the [n.1]MCs.
(24) Fox, M. A.; Shultz, D. A. *J. Org. Chem.* **1988**, *53*, 4386.
(25) Four low-intensity, unresolved peaks: 1333, 1324, 1299, 1265 cm^{-1}. The value used in the text is the average of these four frequencies. The average isotope-induced shift is −16 cm^{-1}.
(26) ^{13}C isotope substitution increases the reduced mass (μ) thereby reducing the vibrational frequency since $\nu(\text{cm}^{-1}) = 4.12(k/\mu)^{1/2}$.

Table II. Variable-Temperature ^{1}H NMR Data for the [*n*.1]MCs[a]

[5.1]MC			[6.1]MC			[7.1]MC[h]		
δH(B)[b]	*T*, °C	*J*,[c] Hz	δH(B)	*T*, °C	*J*, Hz	δH(B)	*T*, °C	*J*, Hz
2.46	26	5.9	2.50	26	*d*	2.52	26	*d*
2.45	0	5.9	2.70, 2.28	0	*d*	2.50	0	*d*
2.44	−10	5.9	2.70, 2.26	−20	13.0, 9.9	2.70, 2.30	−20	*d*
2.43	−20	5.8	2.69, 2.24	−40	13.0, 12.6, 5.5	2.72, 2.22	−40	*d*
2.42	−40	5.8	2.69, 2.24	−60	13.0, 12.6, 5.5	2.72, 2.22	−60	13.8, 4.4, 6.4
2.41	−6	5.5	2.69, 2.24	−80	13.0, 12.6, 5.5	2.72, 2.22	−80	13.8, 4.4, 6.4
2.39	−80	5.2						
δH(HB)[e]			δH(HB)			δH(HB)		
1.40	26	*d*	1.63	26	*d*	1.36	26	5.4
1.39	0	*d*	1.62	0	*d*	1.33	0	5.3
1.38	−10	*d*	1.60	−20	*d*	1.30	−20	5.2
1.46, 1.29	−20	*d*	1.59	−40	*d*	1.28	−40	*d*
1.47, 1.23	−40	*d*	1.57	−60	*d*	1.28	−60	*d*
1.45, 1.21	−60	6.4[f]	1.56	−80	*d*	1.28	−80	*d*
1.44, 1.19	−80	6.4						
δH(BHB)[g]			δH(BHB)			δH(BHB)		
1.07	26	7.2	0.98	26	*d*	0.92	26	*d*
1.05	0	7.2	0.95	0	*d*	0.90	0	*d*
1.04	−10	7.2	0.93	−20	*d*		−20	*d*
1.03	−20	7.2	0.91	−40	*d*	1.02, 0.70	−40	*d*
1.03	−40	7.2	0.89	−60	*d*	0.98, 0.65	−60	*d*
0.99	−60	7.0	0.86	−80	*d*	0.98, 0.65	−80	*d*
0.97	−80	7.0						

[a] Recorded at 500 MHz in deuteriomethylene chloride. Referenced to the residual hydrogens of deuteromethylene chloride at 5.32 ppm. Because the chemical shifts of the tether protons of [4.1]MC show no temperature dependence, they are not included in this table. [b] Chemical shift in ppm of the benzylic protons. [c] H–H coupling constants ±0.1 Hz. [d] Signals are broad and structureless. [e] Chemical shift in ppm of the homobenzylic protons. [f] Average peak separation of a multiplet consisting of at least four lines. [g] Chemical shift in ppm of the bishomobenzylic protons. [h] The trishomobenzylic proton signals appear at 1.12 ppm, J = 6.0 Hz, over the entire temperature range.

Table III. Dihedral Angles, ϕ[a] (degrees), from the X-ray Structures of the [*n*.1]MCs and TPE

ϕ	TPE[b]	[4.1]MC	[5.1]MC	[6.1]MC	[7.1]MC
phenyl torsion[c]	47.76	39.6 (1)	42.9 (3)	45.6 (1)	47.8 (6)
AF	42.89	34.1 (1)	45.3 (3)	46.9 (1)	49.9 (6)
BF	57.05	39.8 (1)	45.2 (3)	44.3 (1)	44.6 (6)
CG	46.10	38.3 (1)	43.4 (3)	46.9 (1)	53.5 (6)
DG	45.01	46.2 (1)	37.8 (3)	44.3 (1)	43.2 (6)
FG[d]	8.44	14.6 (2)	15.1 (4)	15.5 (2)	5.0 (4)

[a] See Figure 1 for definitions of the atomic planes, A, B, C, D, F, and G, which define the dihedral angles, ϕ. Numbers in parentheses are standard deviations in the final digit of the dihedral angle. [b] Reference 22. [c] Average of the phenyl ring torsional angles (AF, BF, CG, DG). [d] Olefinic torsional angle.

Table IV. Bond Lengths (r, angstroms) and Bond Angles (δ,[a] degrees) from the X-ray Structures of the [*n*.1]MCs and TPE

cmpd	$r(\alpha-\alpha')$	$r(1-\alpha)$	r(aromatic)	$\vartheta(1-\alpha-1')$
[4.1]MC	1.348 (4)	1.497 (4)	1.388 (4)	111.0 (2)
[5.1]MC	1.360 (10)	1.497 (12)	1.384 (13)	112.9 (6)
[6.1MC	1.332 (7)	1.484 (5)	1.374 (7)	113.1 (4)
[7.1]MC	1.304 (11)	1.492 (11)	1.372 (13)	111.6 (6)
TPE[b]	1.356	1.496	1.391	114.4

[a] See Figure 1 for definitions of the bond angles. Numbers in parentheses are standard deviations in the final digit(s) of the parameters. [b] Reference 22.

Finally, no large differences between the aromatic C–C and C–H stretching and bending regions of the cyclophanes and tetraphenylethylene were observed.

Excited-State Effects. A. Electronic Absorption Spectra. Table V contains data from the longest wavelength absorption band of the [*n*.1]MCs (the A-band).[27] The corresponding values for the A-band of TTE are included for comparison. The absorption spectra of the [*n*.1]MCs and TTE are shown in Figure 2. There are three significant differences between the A-band of the [*n*.1]MCs and that of TTE. First, the cyclophane A-bands are shifted to longer wavelengths. Second, the cyclophane A-band extinction coefficients are larger. Third, the cyclophane spectral band widths are narrower than those of the model system.

Table V. UV Absorption Spectral Data for the [*n*.1]MCs and TTE[a]

cmpd	λ_{max}[b] (±2), nm	ϵ_{max}[c] (±300), M^{-1} cm^{-1}	$\upsilon_{1/2}$(A)[d] (±350), cm^{-1}	υ_0[e] (±500), cm^{-1}
[4.1]MC	344	15 600	4740	9 950
[5.1MC	340	12 990	4400	10 710
[6.1]MC	340	13 260	4690	10 850
[7.1]MC	324	11 970	5160	11 480
TTE	314	11 200	8190	16 060

[a] Solutions in THF at room temperature. [b] Wavelength maximum of the A-band. [c] Molar extinction coefficient. [d] Width of the A-band measured at half-height. [e] Width of the A-band at the base line.

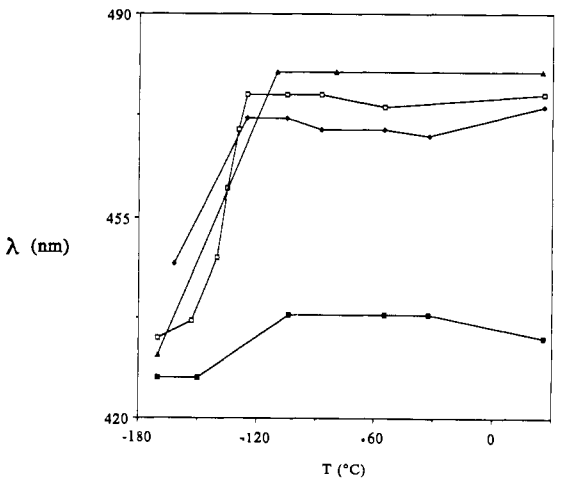

Figure 4. Dependence of fluorescence emission maximum on temperature for the [*n*.1]MCs: ■ [4.1]MC; □ [5.1]MC; ◆ [6.1]MC; ▲ [7.1]MC.

B. Fluorescence Spectra. Emission and excitation spectra of [4.1]MC recorded at 77 K are depicted in Figure 3. All of the cyclophane emission spectra exhibited poorly resolved vibrational structure, at this temperature, and have the same general spectral

(27) The term A-band (conjugation band) was originated by Suzuki; see: Suzuki, H. *Bull. Chem. Soc. Jpn.* **1960**, *33*, 389.

Table VI. Fluorescence Spectral Data for the [*n*.1]MCs and TTE

cmpd	λ_{max}[a] (±2), nm 298 K	77 K	Stokes shift[b] (±250), cm^{-1} 298 K	77 K	Φ_f[c] (±10%)	$\upsilon_{1/2}$(E)[d] (±300), cm^{-1}
[4.1]MC	429	425	6030	5760	0.532	3740
[5.1]MC	469	433	7920	6090	0.029	4150
[6.1]MC	461	445	8180	6890	0.027	4190
[7.1]MC	481	431	9890	7470	≤0.008	4630
TTE	506	431	11380	8440	≤0.001	5300

[a] Wavelength of the fluorescence emission maximum. [b] Measured at 298 and 77 K. [c] Fluorescence quantum yield measured at 26 °C against 9,10-diphenylanthracene. [d] Width of the emission band at half-height.

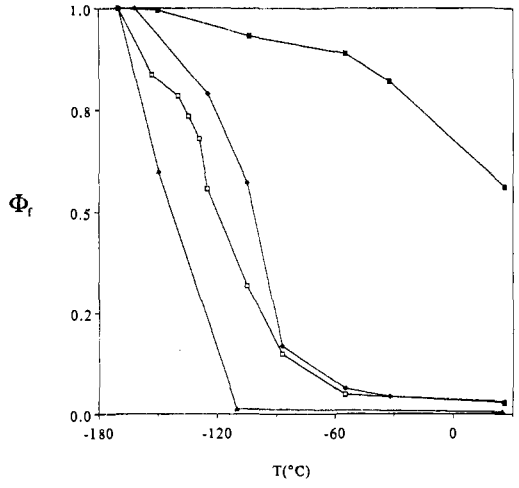

Figure 5. Dependence of fluorescence quantum yield on temperature for the [*n*.1]MCs: ■ [4.1]MC; □ [5.1]MC; ◆ [6.1]MC; ▲ [7.1]MC.

band shape. Excitation spectra are identical with absorption spectra (the A-band) for all compounds in this study. The poorly resolved vibrational structure is absent in the room-temperature spectra except for that of [4.1]MC.[28] As the temperature increases from 77 to 298 K, the emission maxima for all of the compounds shift to longer wavelengths (Table VI and Figure 4), while the excitation maxima remain constant. Values of the emission maxima and Stokes shifts, calculated from the difference in emission and excitation maxima at 298 and 77 K, are listed in Table VI to illustrate the extent of these changes. Emission spectral widths at half-height, $\upsilon_{1/2}$(E), which increase as tether size increases, are also listed in Table VI.

Fluorescence quantum yields (Φ_f) are independent of the excitation wavelength and are listed in Table VI. The Φ_f are temperature dependent and decrease with increasing temperature (Figure 5).[29]

C. Time-Resolved Fluorescence Emission. Upon 355-nm flash excitation of each of the [*n*.1]MCs, we observe a signal attributable to emission from the cyclophane excited singlet state (^{1}v*). The fluorescence observed for [4.1]MC decays exponentially with a rate constant of (5.5 ± 0.5) × 10^8 s^{-1}. The same value of the lifetime of [4.1]MC was measured in single-photon-counting experiments (k_2, Table VII). The decay kinetics observed for [5.1]MC and [6.1]MC are more complex. In both cases, the signals appear to be fit by two first-order processes. Table VII shows the individual rate constants, k_1 and k_2, and the percent of total signal represented by each process, A_1 and A_2. No changes in the decay kinetics outside of experimental error were observed for these signals when polarizers were placed before (set parallel to the incident light) and after (set at the magic angle of 54.7° to the incident light)[30] the sample. The fluorescence decay observed after excitation of [7.1]MC appears to be at least as fast as the pulse width (k_1([7.1]MC) ≥ 3.3 × 10^{10} s^{-1}). Values of the radiative lifetimes estimated from the A-band[31] are also collected in Table VII.

Table VII. Fluorescence Rate Constants[a] for the [*n*.1]MCs and TPE

cmpd	$10^{-8}k_1$, s^{-1}	A_1	$10^{-8}k_2$, s^{-1}	A_2	$10^{-8}k_f$,[b] s^{-1}
[4.1]MC			5.5 ± 0.5		1.97
[5.1]MC	180 ± 20	63 ± 5	26 ± 3	37 ± 3	1.87
[6.1MC	160 ± 20	73 ± 8	35 ± 4	27 ± 3	1.96
[7.1]MC	≥330				2.09
TPE[c]	1700 ± 200				1.82[d]

[a] k_1 = fast component, A_1 = weighting of fast component, k_2 = slow component, A_2 = weighting of slow component, k_f = intrinsic emissive rate constant. [b] Reference 31. [c] Reference 32c. [d] Rate constant measured at 4 K.[32c]

Table VIII. Transient Absorption Decay Rate Constants[a] for the [*n*.1]MCs and TPE

cmpd	$10^{-8}k_{1,T}$,[b] s^{-1}	A_1[b]	$10^{-8}k_{2,T}$	A_2[b]
[4.1MC			5.8 ± 0.8	
[5.1]MC	140 ± 35	69 ± 8	39 ± 5	31 ± 4
[6.1]MC	180 ± 20	80 ± 10	43 ± 6	20 ± 3
TPE[c]	2000 ± 400			
cmpd	$10^{-8}k_{1,TW}$,[d] s^{-1}	A_1[d]	$10^{-8}k_{2,TW}$,[d] s^{-1}	A_2[d]
[4.1]MC			6.0 ± 0.7	
[5.1]MC	138 ± 22	66 ± 8	43 ± 4	34 ± 4
[6.1]MC	190 ± 20	77 ± 10	47 ± 9	13 ± 2

[a] We were unable to observe the ca. 620-nm transient absorption of [7.1]MC; see text for details. [b] $k_{1,T}$ = fast component, A_1 = weighting of fast component, k_{2T} = slow component, A_2 = weighting of slow component, all measured in THF. [c] Reference 32a. [d] $k_{1,TW}$ = fast component, A_1 = weighting of fast component, $k_{2,TW}$ = slow component, A_2 = weighting of slow component, all measured in THF–water (80:20 v/v).

D. Picosecond Absorption Spectroscopy. Upon 355-nm flash excitation of each of the [*n*.1]MCs or TTE, we observe a transient absorption at ca. 430 nm, except for [4.1]MC, whose intense emission (λ_{max} = 429 nm) precluded transient absorption measurements at this wavelength. We attribute these signals to the twisted excited singlet state (^{1}p**).[32a,b] A second transient absorption near 620 nm was observed only for samples of [4.1]MC, [5.1]MC, and [6.1]MC. The 620-nm transient absorption bands of these compounds are shown in Figure 6, parts a–c, respectively. We attribute the 620-nm absorption to the planar excited singlet state (^{1}v*).[32a] The 620-nm transient absorption observed for [4.1]MC decays exponentially with a rate constant of (6.0 ± 0.7) × 10^8 s^{-1} ($k_{2,T}$, Table VIII). As was observed for the fluorescence decays, the transient absorption decay kinetics of [5.1]MC and [6.1]MC exhibit biexponential behavior ($A_{1,T}$, $k_{1,T}$ and $A_{2,T}$, $k_{2,T}$, Table VIII). Rate constants for the growth of the transient absorption at 430 nm are within experimental error of the rate constants for the slow components of the 620-nm transient absorption decays for [5.1]MC and [6.1]MC (i.e., $k_{2,T}$).

To determine the effect of solvent polarity on the ^{1}v* state the cyclophanes, we followed its decay at 620 nm in neat THF and in a THF–water (80:20 v/v) mixture.[33a] As shown in Table VIII,

(28) The spacings between the shoulders on the fluorescence emission spectral envelope are ca. 800 and 1310 cm^{-1}. The interval between the 0,0 transition and the first shoulder on the fluorescence emission spectrum is ca. 1580 cm^{-1}.

(29) We have not attempted to separate viscosity-induced and intrinsic temperature effects. For examples of this see ref 40.

(30) The 54.7° polarizer angle subtracts signals caused by scattered light and/or polarization effects due to molecular tumbling; see: Lakowicz, J. R. *Principles of Fluorescence Spectroscopy*; Plenum: New York, 1983; p 118.

(31) $k_f = 3 \times 10^{-9}\nu_{max}^2 \int \epsilon \delta\nu \approx (3 \times 10^{-9}\nu_{max}^2 \upsilon_0 \epsilon_{max})/2$; see: Turro, N. J. *Modern Molecular Photochemistry*; Benjamin Cummings: Menlo Park, CA, 1978.

(32) (a) Greene, B. I. *Chem. Phys. Lett.* **1981**, *79*, 51. (b) Schilling, C. L.; Hilinski, E. F. *J. Am. Chem. Soc.* **1988**, *110*, 2296. (c) Barbara, P. F.; Rand, S. D.; Rentzepis, P. M. *J. Am. Chem. Soc.* **1981**, *103*, 2156.

(33) (a) We have estimated the E_T value of 80:20 THF–H_2O by first determining the solvent parameter Z and then calculating E_T: $E_T = (Z - 6.92)/1.41$, Z(80:20 THF–H_2O) = 78.14 kcal/mol, and E_T = (78.14 − 6.92)/1.41 = 50.51 kcal/mol. (b) By the relationship between the decay rate constant of the zwitterionic, twisted excited state of tetraphenylethylene and E_T described in ref 32b, we would expect at least a 75-fold increase in the decay rate constant (compared to that in cyclohexane) in 80:20 THF–H_2O. For a discussion of these solvent parameters, see: Reichardt, C.; Dimroth, K. *Fortschr. Chem. Forsch.* **1969**, *11*, 32.

Table IX. Relative Strain Energies of the [*n*.1]MCs, TPE, and TTE

cmpd	SE_{REL},[a] kcal/mol	SE_{arom},[b] %
[4.1]MC	48.8	77
[5.1]MC	26.7	76
[6.1]MC	19.2	71
[7.1]MC	30.8	54
TTE	1.7	
TPE	0.0	

[a] Relative strain energy is defined as the strain energy of the [*n*.1]-MC minus the strain energy of the corresponding tetrakis(*n*-alkylphenyl)ethylene; see Experimental Section. [b] Percent of the strain energy contained in the aromatic portion of the molecule, see Experimental Section.

the decay kinetics in THF–water mixtures (k_{TW}) are identical within experimental error with those in neat THF (k_T).

Discussion

Ground-State Effects. A. NMR Spectra. The order of hydrocarbon tether rigidity of the [*n*.1]MCs may be measured by the temperature dependence (coalescence) of the benzylic (B) CH_2 proton signals. The tether rigidity is greatest for [4.1]MC because these signals are resolved at room temperature. The analogous signals are resolved at −20 °C for [6.1]MC and −60 °C for [7.1]MC and remain unresolved at −80 °C for [5.1]MC. We can therefore estimate rigidity on the basis of the B proton signals in the order [5.1]MC < [7.1]MC < [6.1]MC ≪ [4.1]MC, Table II. However, the homobenzylic (HB) proton signals of [5.1]MC are resolved at a higher temperature (−20 °C) than for either [6.1]MC or [7.1]MC, indicating that rigidity of the tethers is not a simple function of tether size.

Molecular models show that the orientations of the nonbenzylic methylenes of the tethers of [6.1]MC and [7.1]MC may be altered without changing the position of the B CH_2 groups. However, movement of *any* part of the tether [5.1]MC induces movement of the B CH_2 groups.

The H-2 (Figure 1) proton signals of the [*n*.1]MCs shift to higher field as the tether size decreases. This shift is linearly related to both $\vartheta(1-\alpha-1')$ (Table IV) and the average of the phenyl ring torsional angles (Table III). This effect is most likely caused by the distance between H-2 and the neighboring *gem*-phenyl ring, a manifestation of the aromatic "ring-current" effect.[34]

B. Molecular Structure and Strain. Relative strain energies were estimated with MM2[20] force field calculations by subtracting the strain energy of the tetrakis(*n*-alkylphenyl)ethylene from that of the corresponding [*n*.1]MC. These values are listed in Table IX. Approximately 74% of the strain energy is contained in the aromatic framework (as opposed to the tether portions) of the [*n*.1]MCs except [7.1]MC, in which aromatic strain composes only 54% of the total strain energy. The aromatic strain energy is composed mainly of the torsional and bending components which correspond to the largest structural differences between the [*n*.1]MCs and tetraphenylethylene known from X-ray crystal data: the bond angles $\Theta(1-\alpha-1')$ (Table IV), and the phenyl ring torsional angles (Table III) and ethylenic torsional angles (ϕ_{FG}, Table III). The X-ray crystal data also show that the r(aromatic) and $r(1-\alpha)$ bond lengths listed in Table IV are relatively insensitive to tether size. This is consistent with the negligible effect of the tethers on the stretching frequencies in the vibrational spectra. Thus, it appears that the tethers have the greatest effect on bond torsion and bond angle bending.

Excited-State Effects. A. Absorption/Emission Spectra and Vertical Surface Alignment. We attribute the changes in the A-bands of the cyclophanes relative to TTE to their greater rigidity. As the ability of a molecule to distort from its equilibrium geometry is reduced, a better vertical alignment of the ground-state and excited-state surfaces is attained, resulting in red-shifted maxima and larger extinction coefficients for electronic absorptions. These phenomena, as well as narrowing of the absorption

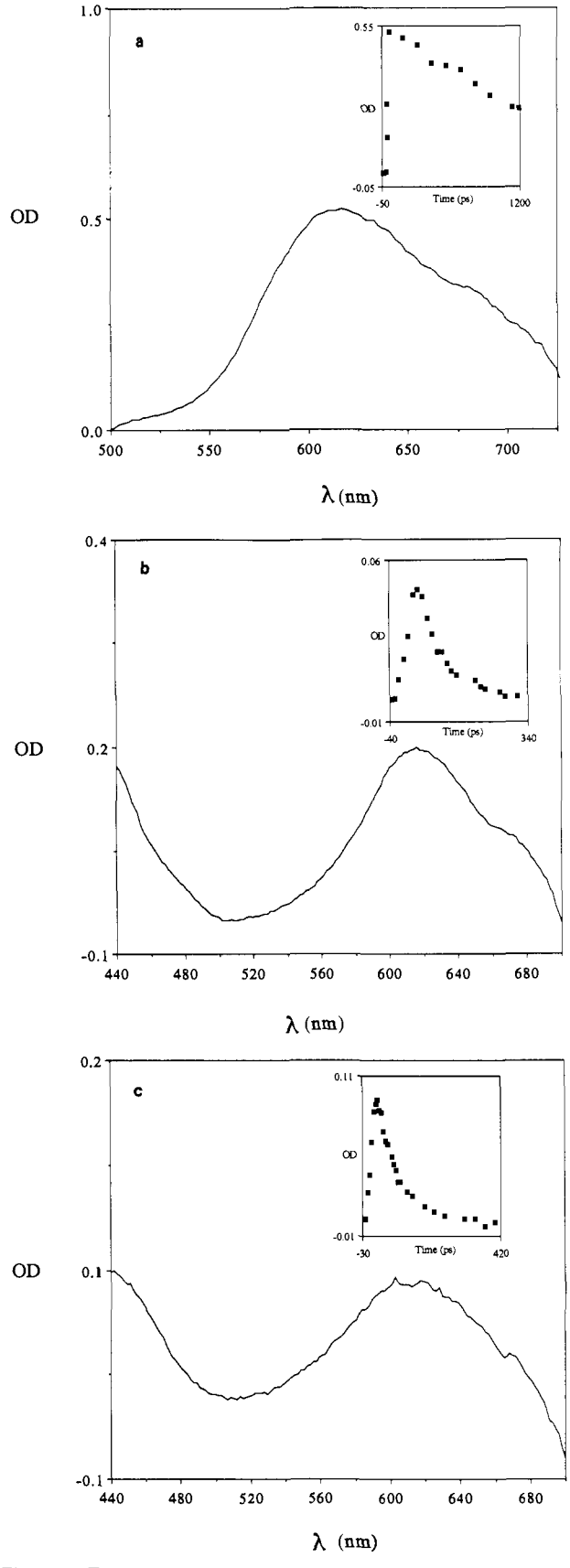

Figure 6. Transient absorption spectra observed following 355-nm excitation: (a) [4.1]MC; (b) [5.1]MC; (c) [6.1]MC. Insets: Decay traces of the ca. 620-nm transient absorption band.

band, are observed for the A-band electronic transitions of the [*n*.1]MCs, Table V. The 0,0 band energy (energy at which the excitation and emission spectra overlap) of the [*n*.1]MCs (74 ± 2 kcal/mol) is identical with that of TTE. Therefore, the red shift

(34) Longuet-Higgins, H. C.; Salem, L. *Proc. R. Soc. London, A* **1960**, *257*, 445. Mallion, R. B. *Mol. Phys.* **1973**, *25*, 1415.

is not caused by a change in the energy gap between the ground-state and excited-state surfaces. Substitution of tetraphenylethylene with four meta-methyl groups (to give TTE) red shifts the A-band only 5 nm, implying that alkyl substitutions cannot explain the observed shifts.

Stokes shifts result from geometry changes in the excited state prior to emission and are therefore a direct measure of vertical alignment of the ground-state and excited-state surfaces. The Stokes shifts of the [*n*.1]MCs are smaller than those of TTE, Table VI. This strongly suggests that the excited-state energy minimum of the cyclophanes is more vertically aligned with the ground-state energy minimum than the corresponding alignment of minima in TTE.

The appearance of unresolved vibrational structure in the fluorescence spectra of the cyclophanes is also consistent with our conclusion that the excited-state and ground-state surfaces of the cyclophanes are more vertically aligned than in TTE. Light emission from an excited state with a geometry different from that in the Franck–Condon region produces ground-state molecules in closely spaced, excited vibrational levels, thus blurring vibrational structure in the emission spectral envelope. The excess vibrational energy in the ground state following emission decreases with decreasing tether size. The spectral manifestation of this is the emission spectral band width at half-height ($\upsilon_{1/2}$(E), Table VI), which decreases as the size of the tether decreases. We suggest that the greater ground-/excited-state alignment is the result of the tether-induced geometry changes discussed earlier, i.e., increased olefinic torsional angles and decreased phenyl ring torsional angles.

Our explanation of the spectral changes in the cyclophanes is consistent with the conclusions reached by Ogawa et al.[35] They analyzed (by considering the nodal properties of the appropriate molecular orbitals) the A-band electronic transitions of several rigid *trans*-stilbene analogues and showed that increases in ethylenic torsional angles and decreases in phenyl ring torsional angles will each lower the energy of this transition (i.e., induce a red shift). These authors interpreted their results in terms of ground-state/excited-state surface alignment (Franck–Condon overlap).[35]

Note that the cyclophanes that exhibit large A-band red shifts have larger olefinic torsional angles (ϕ_{FG}, Table III) and smaller phenyl ring torsional angles (Table III) in agreement with the findings of Ogawa and co-workers.[35] We conclude that the relaxed, vertical singlet excited states of tetraphenylethylenes have slightly increased olefinic torsional angles and decreased phenyl ring torsional angles. The hydrocarbon tethers of the cyclophanes induce these geometric changes, thereby reducing the magnitude of changes that occur once the molecule is in the excited state. Resonance Raman studies on *cis*-stilbene by Myers and Mathies[36] have shown that these same geometric changes occur within 20 fs upon reaching the excited state of *cis*-stilbene.

B. Variable-Temperature Stokes Shifts, Φ_f, and Emission Maxima as a Measure of Molecular Rigidity. Stegemeyer,[37] Fischer et al.,[38] and Sharafy and Muszkat[39] have attributed the low-temperature-induced blue shift of arylethylene emission to the limitation of the amplitudes of various torsional and out-of-plane vibrations by high viscosities of solvents at low temperatures. Phenyl ring torsional restrictions, inherent in the [*n*.1]MCs, are the same as those of nontethered arylethylenes in viscous solvents or frozen glasses. The relative magnitudes of these restrictions may be evaluated by examining the emission maxima, Stokes shifts, and Φ_f as a function of temperature.

The temperature dependence of emission maxima of the cyclophanes is a function of tether size, Figure 4, with smaller shifts being observed, in general, for smaller tethers. There is only a small difference between the Stokes shifts at 298 K and that at 77 K for [4.1]MC (270 cm^{-1}), which is consistent with its rigid structure. However, there is a large difference between the Stokes shift at 298 K and that at 77 K for [5.1]MC, [6.1]MC, and [7.1]MC. The large difference in Stokes shifts of [5.1]MC (1830 cm^{-1}) compared to [6.1]MC (1290 cm^{-1}) implies that the magnitude of flexibility in [5.1]MC is greater than in [6.1]MC. [7.1]MC shows the largest differences in emission maxima and Stokes shifts between room temperature and 77 K.

The fluorescence spectrum of [4.1]MC at 298 K is much the same as that of TTE measured at 77 K. An analogous observation has been made for *trans*-stilbene and a rigid stilbene derivative, *trans*-1,1′-biindanylidene, which exhibits resolved vibrational structure in its room-temperature absorption spectrum.[40] However, the fluorescence quantum yield of the more rigid[41] *trans*-1,1′-biindanylidene is at least 20 times lower than that of *trans*-stilbene, in marked contrast to the [*n*.1]MCs, which are more fluorescent than their non-tethered counterpart, TTE. The tethers of the cyclophanes that control phenyl ring torsion in the ground state *inhibit* further, apparently critical, decreases in these torsional angles in the excited state. Indeed, Saltiel and D'Agostino have suggested that the rate of olefinic twisting may be enhanced for *smaller* phenyl ring torsional angles.[40] Large tethers (e.g., those of [7.1]MC) do not inhibit decreases in phenyl ring torsional angles in the excited state, and therefore these cyclophanes show only small increases in Φ_f.

At room temperature, the fluorescence efficiency of [4.1]MC is over 500 times that of TTE, Table VI. [5.1]MC and [6.1MC are 30 times more emissive than TTE, and [7.1]MC is almost an order of magnitude more emissive than TTE. The plots of Φ_f vs temperature for the [*n*.1]MCs show that somewhat lower temperatures are required for solutions of [7.1]MC than for [5.1]MC and for [6.1]MC to observe the same value of Φ_f, Figure 5. Thus, the temperature-dependent Stokes shifts, emission maxima, and Φ_f values all indicate that molecular rigidity increases as the tether size decreases, with the exception of [5.1]MC.

C. Time-Resolved Spectra. The results of the time-resolved experiments discussed below provide direct spectroscopic evidence that the phenyl ring torsional restrictions of the [*n*.1]MCs impede olefinic torsion in the excited state.

Time-Resolved Fluorescence Emission. Previously, we reported the fluorescence polarization ratios[42] of the [*n*.1]MCs and TTE.[4] The fluorescence polarization ratios of [5.1]MC and [6.1]MC were found to be intermediate between those of [4.1]MC and TTE and to increase in the order TTE > [6.1]MC > [5.1]MC > [4.1]MC. Since the fluorescence polarization ratio is inversely proportional to the excited-state lifetime,[37] we concluded that the excited-state lifetimes of the [*n*.1]MCs should be significantly longer than that of tetraphenylethylene. The time-resolved emission studies presented here show this to be the case.

As shown in Table VII, all the cyclophane vertical excited states decay much more slowly than the excited state of tetraphenylethylene. [4.1]MC appears to decay exponentially while [5.1]MC and [6.1]MC do not; the decay of their emission could, however, be fit as two first-order processes. This implies that at least two kinetically distinct species are formed in the excited states of [5.1]MC and [6.1]MC. We suggest that these non-interconvertible species are conformers, differentiated by their phenyl ring torsional amplitudes. This interpretation is similar to a previous report in which the wavelength-dependent fluorescence of tetraphenylethylene was attributed to different torsionally induced radiationless decays.[32c] The fluorescence decay of [7.1]MC is too fast for accurate kinetic analysis, indicating that the additional

(35) Ogawa, K.; Suzuki, H.; Futakami, M. *J. Chem. Soc., Perkin Trans. 2* **1988**, 39.

(36) Myers, A. B.; Mathies, R. A. *J. Chem. Phys.* **1984**, *81*, 1552. See also: Myers, A. B.; Trulson, M. O.; Mathies, R. A. *J. Chem. Phys.* **1985**, *83*, 5000.

(37) Stegemeyer, H. *Ber. Bunsen-Ges. Phys. Chem.* **1968**, *72*, 335.

(38) Fischer, G.; Seger, G.; Muszkat, K. A.; Fischer, E. *J. Chem. Soc., Perkin Trans. 2* **1975**, 1569.

(39) Sharafy, S.; Muszkat, K. A. *J. Am. Chem. Soc.* **1971**, *93*, 4119.

(40) Saltiel, J.; D'Agostino, J. T. *J. Am. Chem. Soc.* **1972**, *94*, 6445.

(41) For an additional viewpoints concerning the geometry and photophysics of *trans*-1,1′-biindanylidene (as well as the cis isomer), see: (a) Vogel, J.; Schneider, S.; Dörr, F.; Lemmen, P.; Lenoir, D. *Chem. Phys.* **1984**, *90*, 387. (b) Lemmen, P.; Lenoir, D. *Chem. Ber.* **1984**, *117*, 2300.

(42) Fluorescence polarization ratio, $P = (I_{\parallel} - I_{\perp})/(I_{\parallel} + I_{\perp})$, where $I_{\parallel}$ ($I_{\perp}$) is the intensity of emission parallel (perpendicular) to the plane-polarized excitation light.

torsional freedom allowed by the seven-carbon tether enhances deactivation of the excited singlet state relative to the other cyclophanes and approaches that of tetraphenylethylene.

The tether-induced torsional restrictions in the [*n*.1]MCs drastically affect the photophysics of tetraphenylethylenes. The increase in Φ_f in the cyclophanes may be caused by either an increase in k_f (Table VIII) or a decrease in the sum of the excited-state deactivation processes. We propose that the increase Φ_f observed for the cyclophanes is not caused by an increase in k_f based on the following observations. The fastest process that deactivates the excited state of tetraphenylethylene is cis–trans isomerization, $k_{CT} > 1.8 \times 10^{11}$ s^{-1}.[2,32c] The second fastest process of tetraphenylethylene excited-state decay is formation of 4a,4b-dihydro-9,10-diphenylphenanthrene, $\Phi_{DHP} \cong 0.022$, $k_{DHP} \approx 4 \times 10^9$ s^{-1}.[32c,43] Photochemical product formation from the [*n*.1]MCs accounts for less than 2% of the excited-state decay processes.[44] Since the rate of intersystem crossing for tetraphenylethylene is negligible,[45] these observations imply that it is k_{CT} that is attenuated in the [*n*.1]MCs. Thus, either the activation barrier or the pre-exponential A_1 factor for olefinic twisting is substantially increased by restricting phenyl ring torsion.

Picosecond Absorption Spectra. Direct spectroscopic evidence of a long-lived, planar excited state of the [*n*.1]MCs is provided by picosecond absorption spectroscopy discussed below.

Greene observed four spectroscopically distinct relaxation processes in a recent study of the transient absorption spectrum of tetraphenylethylene.[32a] A transient absorption at ca. 640 nm was attributed to the planar, fluorescent excited singlet state (^{1}v*) of tetraphenylethylene which decayed with a lifetime of 5 ± 1 ps. A second absorption at 423 nm was ascribed to the nonfluorescent α–α' twisted state (^{1}p**). This absorption band which was blue shifted and narrowed on a time scale of 400 ps, decayed with a lifetime of 3.0 ± 0.5 ns. The spectral narrowing was attributed to phenyl ring rotation. The results of time- and wavelength-resolved fluorescence decay studies of tetraphenylethylene by Barbara et al.[32c] were interpreted as evidence for the involvement of at least two distinct torsional relaxation processes. Schilling and Hilinski[32b] have recently shown that the tetraphenylethylene ^{1}p**-state transient absorption decay rate is linearly dependent on the solvent parameter E_T. They suggest that this solvent dependence is evidence that the tetraphenylethylene ^{1}p** state possesses zwitterionic character characteristic of a doubly excited species, in agreement with theoretical predictions.[5,46]

The 620-nm transient absorption bands of the [*n*.1]MCs are slightly blue shifted (ca. 20 nm) relative to that of tetraphenylethylene and decay on a much longer time scale. We assign the cyclophane transient absorptions at 430 and 620 nm to the ^{1}p** and ^{1}v* states, respectively, based on their similarity with previous observations.[32a,b] The concomitant decay of absorption at 620 nm and growth of absorption at 430 nm indicate that the ^{1}v* state decays to the ^{1}p** state. As observed for the fluorescence decay, the 620-nm transient absorption bands of [5.1]MC and [6.1]MC decay by at least two first-order processes. Because the rate constants for fluorescence decay are within experimental error of the rate constants for decay of the 620-nm transient absorption (Tables VII and VIII, respectively), both of these processes correspond to the same excited state.

To assess the electronic character (diradicaloid or zwitterionic) of the fluorescent state of the [*n*.1]MCs, we measured the 620-nm transient absorption decay in two solvents, THF and 80:20 (v/v) THF–H_2O. Since the decay kinetics of this absorption are not affected by solvent polarity (Table VIII),[33b] we suggest that the ^{1}v* state has primarily diradicaloid[5g] character. Also, the transition

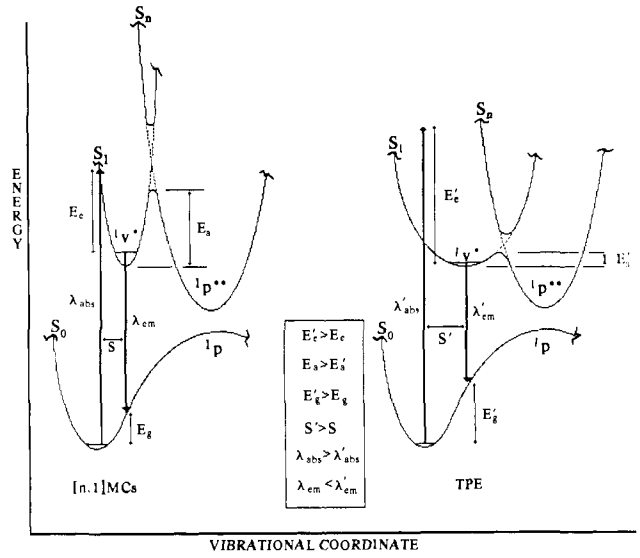

Figure 7. Qualitative diagram of the potential energy curves for the [*n*.1]MCs and tetraphenylethylene (TPE) summarizing the observed data. Primed parameters refer to tetraphenylethylene, while those without a prime refer to the [*n*.1]MCs. E_e = excited-state relaxation, E_a = energy barrier for ^{1}v* to ^{1}p** surface crossing, E_g = ground state relaxation, S = Stokes shift, λ_{abs} = absorption maximum, λ_{em} = emission maximum.

state of the ^{1}v* to ^{1}p** surface crossing apparently occurs at a point in which there is little charge separation in the zwitterionic, ^{1}p** state (i.e., at a small olefinic torsional angle); therefore, solvent polarity does not affect the height of the energy barrier. If the ^{1}p** state of the [*n*.1]MCs is a doubly excited zwitterionic state as is tetraphenylethylene,[32b] we suggest that these and previous[32b] results provide physical evidence for an electronic surface crossing from ^{1}v* to ^{1}p**.

D. [*n*.1]MC Excited-State Surfaces. The shape of an excited-state potential energy surface can be estimated by examining the electronic absorption spectrum. An absorption spectrum may be calculated by considering the overlap of the excited-state wave function immediately after excitation with that at some time following motion on the excited state Born–Oppenheimer potential energy surface.[47a,b] Motion on the excited-state surface is related to the width of the absorption band at half-height ($\upsilon_{1/2}$(A), Table V). A broad absorption band will be observed if the excited-state surface motion is fast; i.e., a large $\upsilon_{1/2}$(A) implies a steep excited-state surface. A narrow absorption band is the result of slow translation on the excited-state surface; i.e., a small $\upsilon_{1/2}$(A) requires a shallow excited-state surface.[47]

A classical description of excited-state surface shape and excited-state decay has been used by Fischer and co-workers.[38] Using CFF-SCF-PI-CI calculations,[48] they showed that *cis*-stilbene (broad absorption band), because of its nonpolar geometry, has a considerably greater density of vibrational levels in the excited state and more excited-state normal modes with large gradients than does *trans*-stilbene (narrow absorption band). This causes

(43) Olsen, R. J.; Buckles, R. E. *J. Photochem.* **1981**, *10*, 215.
(44) Irradiated benzene solutions of the [*n*.1]MCs containing iodine[43] were unchanged after 10–20% consumption of tetraphenylethylene had occurred.
(45) Görner, H. *J. Phys. Chem.* **1982**, *86*, 2028.
(46) For discussions of calculations of stilbene excited-state surfaces, see: (a) Orlandi, G.; Siebrand, W. *Chem. Phys. Lett.* **1975**, *30*, 352. (b) Tavan, P.; Schulten, K. *Chem. Phys. Lett.* **1978**, *56*, 200. (c) Gregory, R. A.; Williams, D. F. *J. Phys. Chem.* **1979**, *83*, 2652. (d) Orlandi, G.; Palmieri, P.; Poggi, G. *J. Am. Chem. Soc.* **1979**, *101*, 3492.
(47) For papers on the relationship between electronic absorption spectra and excited-state surface shapes/dynamics, see the following: (a) Heller, E. *Acc. Chem. Res.* **1981**, *14*, 368, and references cited therein. (b) Heller, E.; Sundberg, R. L.; Tannor, D. *J. Phys. Chem.* **1982**, *86*, 368. (c) Campion, P. M.; Albrecht, A. C. *Annu. Rev. Phys. Chem.* **1982**, *33*, 353. (d) Warshel, A.; Dauber, P. *J. Chem. Phys.* **1977**, *66*, 5477. (e) Chadwick, R. R.; Gerrity, D. P.; Hudson, B. S. *Chem. Phys. Lett.* **1985**, *115*, 24. (f) Patapoff, T. W.; Turpin, P.-Y.; Peticolas, W. L. *J. Phys. Chem.* **1986**, *90*, 2347. (g) Sue, J.; Yan, Y. J.; Mukamel, S. *J. Phys. Chem.* **1986**, *85*, 462. (h) Ziegler, L. D.; Varotsis, C. *Chem. Phys. Lett.* **1986**, *123*, 175. (i) Hale, M. O.; Galica, G. E.; Glogover, S. G.; Kinsey, J. L. *J. Phys. Chem.* **1986**, *90*, 4997. (j) Myers, A. B.; Harris, R. A.; Mathies, R. A. *J. Chem. Phys.* **1983**, *79*, 603. (k) Myers, A. B.; Trulson, M. O.; Pardoen, J. A.; Heeremans, C.; Lugtenburg, J.; Mathies, R. A. *J. Chem. Phys.* **1986**, *84*, 633, and ref 36.
(48) (a) Warshel, A.; Karplus, M. *J. Am. Chem. Soc.* **1972**, *95*, 5612. (b) *Ibid.* **1974**, *96*, 5677. (c) Warshel, A.; Karplus, M. *Chem. Phys. Lett.* **1972**, *17*, 7.

the rate constant for radiationless decay of the *cis*-stilbene excited state to be greater than that of *trans*-stilbene.[2,38,47k,49]

The lower density of vibrational states in the excited state of the [*n*.1]MCs relative to TTE is demonstrated by the smaller absorption spectral widths υ_0(A), Table VI, of the [*n*.1]MCs. This lower density of vibrational states results in slower vibrational relaxation in the [*n*.1]MCs relative to TTE.

A qualitative diagram of the excited-state and ground-state surfaces of tetraphenylethylenes and the [*n*.1]MCs, whose shapes and surface slopes are consistent with the absorption and fluorescence emission spectral data and time-resolved measurements, is given in Figure 7. The excited-state potential energy surface of the [*n*.1]MCs is considerably more sloped than the excited-state potential energy surface of tetraphenylethylene. The shallow potential energy well of tetraphenylethylene contains a higher density of vibrational levels (larger υ_0(A)) than does the steep potential well (smaller υ_0(A)) of the [*n*.1]MCs. This simple diagram thus explains the red shift of the A-bands of the [*n*.1]-MCs, the decrease in the Stokes shift exhibited by the cyclophanes, and the blue shift of the fluorescence emission maximum. Figure 7 also indicates that passing over the energy barrier is accompanied by an electronic-state surface crossing.

The difference in photophysical behavior between the [*n*.1]MCs and TTE is that both the steeper excited-state slope of the [*n*.1]MCs and the better alignment of these surfaces may cause an increase in the activation barrier (E_a) for eventual radiationless decay (cis-trans isomerization). Using the Arrhenius *A* value for stilbene ^{1}v* decay,[5d] the rate constant for TPE fluorescence decay,[32c] and $\Phi_{CT} \approx 0.95$,[2] we estimate that the increase in the excited-state surface slope of the cyclophanes causes E_a to increase from ca. 1.8 kcal/mol (tetraphenylethylene) to ca. 5.6 kcal/mol ([4.1]MC). Alternatively, if E_a([4.1]MC) = E_a(TPE) $\cong$ 1.8 kcal/mol, the Arrhenius *A* value for [4.1]MC must decrease from ca. 4.4×10^{11} (ref 5d) to ca. 6×10^9 s^{-1}. Thus, the increased slope of the excited-state potential well of the cyclophanes, caused by restricting phenyl ring torsion, reduces the rate of cis–trans isomerization.

Conclusions

The similarities in the vibrational spectra and bond lengths, deduced from X-ray crystallographic data, between the [*n*.1]MCs and tetraphenylethylene show that the tethers do not affect these parameters. However, the hydrocarbon tethers of the [*n*.1]MCs do affect olefinic and phenyl ring torsion as indicated by analysis of NMR and electronic absorption/emission spectra and X-ray crystallographic data. The magnitude of this effect is approximately proportional to the size of the tether. These tether-induced geometric changes dramatically affect the photophysical properties of tetraphenylethylenes.

Two observations indicate that the limit of phenyl ring torsional freedom required to approximate "tetraphenylethylene-like" behavior is approached by [7.1]MC. First, the fluorescence decay rate of [7.1]MC is intermediate between that of [6.1]MC and tetraphenylethylene. Second, we do not observe a transient absorption attributed to the planar excited state of [7.1]MC, which is observed for other members of this family with shorter tethers, indicating that isomerization efficiency is decreased if the tether is composed of less than seven carbons. Also, it appears that the shorter five carbon tether does not impose as much rigidity as a longer six carbon tether.

We suggest that the largest contributor to singlet excited-state deactivation is phenyl ring torsion rather than olefinic torsion. Finally, our experimental observations are consistent with an electronic surface crossing from a nonpolar ^{1}v* state to the zwitterionic ^{1}p** state that eventually leads to cis–trans isomerization.

Additional work on the photochemistry of the [*n*.1]MCs, as well as studies to determine the effect of phenyl ring torsional restraint on the redox properties of tetraphenylethylenes, is underway.

Acknowledgment. This work was supported by the Office of Basic Energy Sciences Division of Chemical Sciences, U.S. Department of Energy and by the Robert A. Welch Foundation. We thank E. Gaillard, and Dr. S. Atherton for helpful suggestions and discussions, as well as Dr. J. G. Radziszewski for recording the FT Raman spectra, S. Sorey for the variable-temperature NMR work, Drs. S. Hubig and S. Atherton of the Center for Fast Kinetic Research (CFKR) for their help in obtaining the picosecond absorption and time-resolved fluorescence data, V. Lynch for the crystallographic analysis, and K. Worthen for obtaining the differential scanning calorimetric results. CFKR is a user facility supported by the National Institutes of Health (DRR 00886) and by the University of Texas at Austin.

Supplementary Material Available: ORTEP plots of the [*n*.1]MCs (4 pages); listing of X-ray structure factor amplitudes (105 pages). Ordering information is given on any current masthead page.

(49) The rate constant for radiationless decay, $k_d = 2\pi/hJ^2\rho F(E)$ (where $F(E)$ is related to the number of excited vibrational levels produced upon electronic excitation) see: (a) Burland, D. M.; Robinson, G. W. *J. Chem. Phys.* **1969**, *51*, 4548. (b) Siebrand, W. *J. Chem. Phys.* **1967**, *46*, 440.